

Scanning tunneling microscopy and spectroscopy investigations of QCA molecules

M. Manimaran^{a,*}, G.L. Snider^a, C.S. Lent^a, V. Sarveswaran^b, M. Lieberman^b,
Zhaohui Li^b, T.P. Fehlner^b

^aDepartment of Electrical Engineering, University of Notre Dame, Notre Dame, IN 46556, USA

^bDepartment of Chemistry and Biochemistry, University of Notre Dame, Notre Dame, IN 46556, USA

Received 29 May 2002; received in revised form 28 February 2003

Abstract

Quantum-dot cellular automata (QCA), a computation paradigm based on the Coulomb interactions between neighboring cells. The key idea is to represent binary information, not by the state of a current switch (transistor), but rather by the configuration of charge in a bistable cell. In its molecular realization, the QCA cell can be a single molecule. QCA is ideally suited for molecular implementation since it exploits the molecule's ability to contain charge, and does not rely on any current flow between the molecules. We have examined using an UHV-STM some of the QCA molecules like silicon phthalocyanines and Fe–Ru complexes on Au (1 1 1) and Si (1 1 1) surfaces, which are suitable candidates for the molecular QCA approach.

© 2003 Elsevier Science B.V. All rights reserved.

Keywords: Scanning tunneling microscopy; Quantum-dot cellular automata; Silicon phthalocyanine; Fe–Ru complex; Molecular electronics

1. Introduction

The developing technology of quantum dot fabrication may prove a key element in crafting another approach for quantum computing [1]. Most approaches to molecular electronics have sought to reproduce conventional electronic elements, such as transistors, wires, or diodes. To this date, no one has demonstrated a molecular electronic device that functions in concert with others. As in conventional electronics, connecting the device components is a major problem.

It is prudent, then, to search for a replacement paradigm for computing which does not rely on power hungry transistors and relatively slow metal interconnects. The computational paradigm known as quantum-dot cellular automata (QCA) is one such possibility [2].

QCA is completely a new architecture for computation, which is based on encoding binary information in the charge configuration of quantum-dot cells. The information is transmitted between QCA cells through Coulomb interactions depending on the arrangement of the cells. Bits can be transmitted, inverted, or processed with logic operations (AND, OR). Information processing does not require the flow of current, so QCA has

*Corresponding author.

E-mail address: maran@ibn.a-star.edu.sg (M. Manimaran).

the potential for extremely low power dissipation. No current flows between cells and any power or information are delivered to individual internal cells. Local interconnections between cells are provided by the physics of cell–cell interaction. The basic concept of QCA cell operation is given in Fig. 1. Orlov et al. [3] have fabricated and tested the clocked single-electron switching in QCA based on metal dots on an oxidized silicon substrate at below liquid-helium temperature. They have demonstrated that a clock signal can be used to control the charge state of the QCA cell. These metal dot tunnel-junction cells operate at 80 mK, but even within the metal tunnel-junction paradigm it is clear that as sizes of dots and junctions shrink, operating temperatures increase. Molecular scales (~ 2 nm) are predicted to yield room temperature QCA operation. The QCA approach exploits the molecule as a structured charge container. One molecule's state is communicated to its neighbors through Coulomb forces.

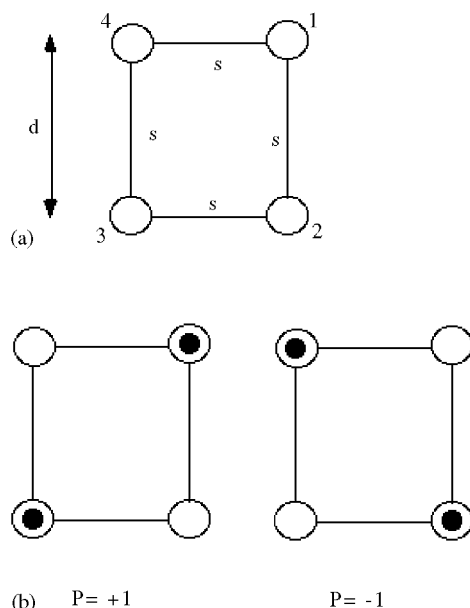


Fig. 1. Schematic of the basic four-site cell: (a) The geometry of the cell. The tunneling energy between two neighboring sites is designated by s , while d is the near-neighbor distance. (b) Coulombic repulsion causes the electrons to occupy antipodal sites within the cell. The two bistable states result in cell polarization of $P = +1$ and -1 (see Ref. [2]).

Remarkably, this interaction is sufficient to enable general-purpose computing. There is a key place for current-carrying molecules in the QCA paradigm—as inputs and electrometers. Electrometers are necessary to sense the state of output cells and communicate this information to the macroscopic world. These detectors could then be coupled to CMOS amplifiers to bring signal levels up [4].

While molecular implementations present many serious challenges, particularly in input and output, they have the advantages of perfectly uniform cell size and enormous numbers of cells on which to experiment. In this work, we have examined using the UHV scanning tunneling microscopy (STM), the possibility of silicon phthalocyanines (SiPcs) and $[\text{Ru}(\text{dppm})_2(\text{C}\equiv\text{CFc})(\text{C}\equiv\text{CPhOCH}_3)]$ (herein after referred as FeRu(OCH₃) complex) and $[\text{Ru}(\text{dppm})_2(\text{C}\equiv\text{CFc})(\text{N}\equiv\text{CCH}_2\text{CH}_2\text{NHC}(\text{O})(\text{CH}_2)_n\text{SH})][\text{PF}_6]$ (herein after referred as FeRu (SH) complex, where $n = 3, 10, 16$ but in this work $n = 3$) as the potential candidates for this molecular QCA approach.

The phthalocyanines (Pcs) may play an important role in new electronic devices due to their useful optical and electronic properties [5]. There are other chemical properties, which make SiPc a potential candidate for QCA. For example, SiPc can act as structural building blocks in monolayer and multilayer films. Also, the axial ligands of the SiPcs are easy to modify so that these molecules can be attached to different substrates. The eight pentyloxy groups available in SiPc makes it soluble in organic solvents, which paves the way for the characterization and solution studies.

Molecules with ferrocene (Fc) containing complexes like Fe–Ru complex are of great interest owing to the rapid growth of materials science. This system is similar to one reported by Touchard et al. [6]. By introducing another metal in close proximity to the metallocenyl complex gives a wider diversity of oxidation states and ligands, which increase the possible architectural flexibility and fine-tuning of the properties essential for electronic device applications. In particular, Fe–Ru complex exhibits two oxidation waves and the singly oxidized complex rouse properties of a mixed valence complex. The purpose of the attachment of this compound to the surface is to

study single molecule switching by vertical electron transfer.

STM allows us to visualize the molecular nanostructures and to study redox processes in the single molecules with high spatial and spectral resolution at ambient and UHV conditions. The molecular structure of samples for the investigation of single redox centers by this technique must be a monolayer on the conducting substrate [7]. Until now, however, no one has studied the morphology of these QCA molecules by STM. In this paper, we present the experimental results on the STM characterization of these monolayer QCA molecules on Au and Si substrates. The obtained experimental data on the STM study of morphology give evidence for the presence of these molecules on the substrates.

2. Experimental

2.1. Preparation of silicon phthalocyanine (SiPc) monomer and dimer

2.1.1. Synthesis of SiPc monomer [MeSiPc(OC₅H₁₁)₈OSiCl₃] (referred as *m*-SiPc)

For the synthesis of monomer, the methods proposed by Hanack and Kenney et al. were adopted [8,9]. Soluble SiPc with eight peripheral pentyloxy groups were synthesized from the corresponding disubstituted diiminoisindolines [10]. For dipentyloxydiiminoisindoline, catechol was first brominated, and then the phenolic oxygen was coupled to pentyl bromide under basic conditions to give dibromodipentyloxybenzene. The yield was 76% from catechol. The aromatic bromide was then substituted by cyanide in a Sandmeyer reaction with a typical yield of 40–60%, and the resulting phthalonitriles were converted into diiminoisindolines by addition of gaseous ammonia in methanol. Copper phthalocyanines were obtained as a side product in the Sandmeyer reaction. Methylchloro SiPcZ₈ (Z = pentyloxy) was made by refluxing disubstituted diiminoisindoline and excess MeSiCl₃ in dry quinoline for about an hour. The green precipitates were then washed with dry acetonitrile in a Soxhlet extractor under Ar for 24 h to remove

any impurities. The isolated yield for this condensation varies from 30% to 50%. The axial Si–Cl bond in these SiPcs is extremely sensitive to water, which yields [MeSiPc(OC₅H₁₁)₈OH] and this product reacts with SiCl₄ in the presence of pyridine to yield the monomeric MeSiPc(OC₅H₁₁)₈OSiCl₃. The schematic diagram of the reaction process of monomer synthesis is given in Fig. 2(a).

2.1.2. Synthesis of SiPc dimer

[(HSCH₂CH₂O)SiPc(OC₅H₁₁)₈]₂O (referred as *d*-SiPc)

As reported earlier by Li et al. [11], oxo SiPc dimers were synthesized in a sealed tube by dehydration of MeSiPc(OC₅H₁₁)₈OH in benzene in the presence of pyridine. The temperature of 150–165°C needed for this dimerization in the octasubstituted SiPcs was lower than the 190°C solid-phase reaction required for unsubstituted SiPcs reported by Kenney and others [12]. Furthermore, only dimers are formed in this solution phase condensation. The stable Si–Me axial cap prevents formation of higher oligomers, such as trimers or tetramers. The octapentyloxy substituted SiPc dimerized at 150°C in 12 h with isolated yield of 40%. The [Me(SiPc)(OC₅H₁₁)₈]₂O (10 mg) and excess mercaptoethanol in deuterated benzene (C₆D₆) were photolyzed at 350 nm in a Raynet photochemical reactor for 40 min to get the desired dimer [HSCH₂CH₂O(SiPc)(OC₅H₁₁)₈]₂O in 40% yield as shown in Fig. 2(b).

2.2. Preparation of FeRu(OCH₃) and FeRu(SH) complexes

2.2.1. Synthesis of

[Ru(dppm)₂(C≡CFc)(C≡CPhOCH₃)] (referred as *FeRu(OCH₃) complex*)

The preparation of [Ru(dppm)₂(C≡CFc)(C≡CPhOCH₃)] is shown in Fig. 3(a). [RuCl(dppm)₂(C≡CFc)] (112 mg, 0.1 mM), HC≡CPhOCH₃ (20 μl), NaPF₆ (17 mg, 0.11 mM) and NEt₃ (40 μl) were stirred in CH₂Cl₂ (20 ml) for 12 h. The resultant brown solution was filtered and DBU (20 μl) was added into it. The color changed from brown to orange immediately. It was stirred for another 2 h and was dried in vacuum. After that

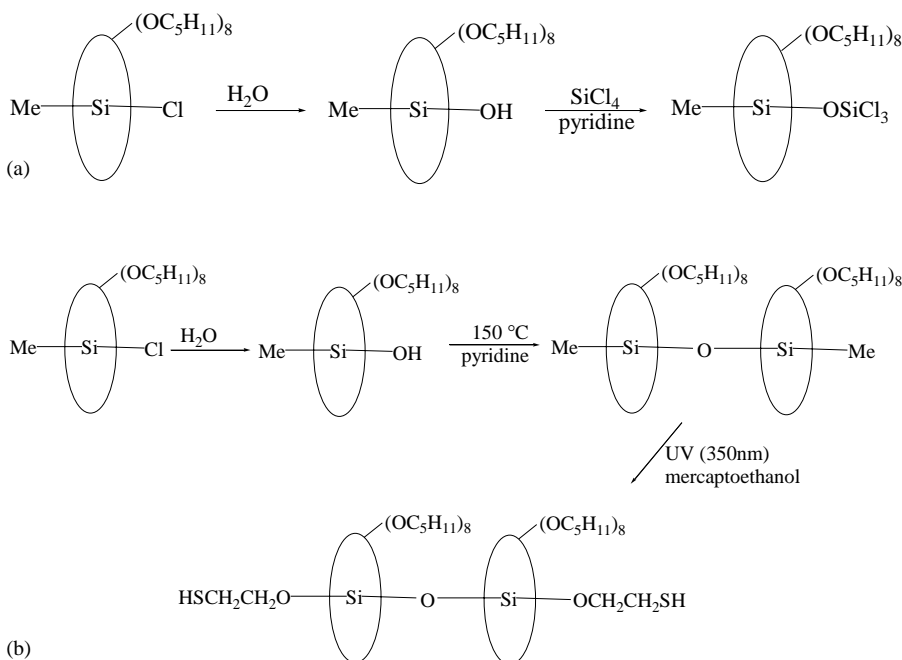


Fig. 2. The schematic diagram of the preparation of (a) SiPc monomer for Si surface (b) SiPc dimer for Au surface.

the product was purified by running through an Al_2O_3 column using CH_2Cl_2 :ether (2:1) as elute. Golden needle crystals of $\text{FeRu}(\text{OCH}_3)$ were obtained from CH_2Cl_2 :ether (1:3) solution. The resultant $\text{FeRu}(\text{OCH}_3)$ crystals were then used in the preparation of the monolayer on Si substrate.

2.2.2. Synthesis of

$[\text{Ru}(\text{dppm})_2(\text{C}\equiv\text{CFc})(\text{N}\equiv\text{CCH}_2\text{CH}_2\text{NHC}(\text{O})(\text{CH}_2)_n\text{SH})][\text{PF}_6]$ (referred as *FeRu(SH) complex*)

As shown in Fig. 3(b), the $[\text{Ru}(\text{dppm})_2(\text{C}\equiv\text{CFc})(\text{N}\equiv\text{CCH}_2\text{CH}_2\text{NH}_2)][\text{PF}_6]$ (referred as *FeRu(NH₂) complex*) was first prepared by adding together $[\text{RuCl}(\text{dppm})_2(\text{C}\equiv\text{CFc})]$ (60 mg, 0.053 mM), TIPF_6 (20 mg, 0.058 mmol) and $\text{N}\equiv\text{CCH}_2\text{CH}_2\text{NH}_2$ (40 μl , excess) in CH_2Cl_2 (10 ml). The resultant suspension was stirred at room temperature for 15 h. After that the suspension was filtered and the orange filtrate was dried in vacuum to get an orange powder substance. The orange powder obtained was then washed with ether and recrystallized from CH_2Cl_2 :ether solution (1:3) to yield the orange crystals of *FeRu(NH₂) complex*. In

order to attach the thiol tail with this molecule so as to attach it directly on the Au surface, the following method was adopted. *FeRu(NH₂)*, DCC and $\text{HS}(\text{CH}_2)_n\text{COOH}$ in 1:1:1 ratio was stirred in CH_2Cl_2 for overnight. After that the yellow suspension was filtered and the yellow filtrate was dried in vacuum. The desired *FeRu(SH)* complex was obtained by recrystallization from CH_2Cl_2 :ether (1:3) solution. The resultant *FeRu(SH)* crystals were then used in the preparation of the monolayer on Au substrate.

2.3. Molecule attachment on Au (111) and Si (111) surfaces for STM imaging

For the molecule attachment on the Au and Si surfaces, the following methods were adopted. The commercially available Au (111) single crystal film, approximately 1500 Å thick purchased from the Molecular Imaging Inc., was flame annealed with hydrogen at 800 °C and cleaned with CH_2Cl_2 , acetone, and isopropyl alcohol (IPA) and rinsed with DI H_2O followed by drying in a N_2 gas stream. For the attachment of molecules on the Si

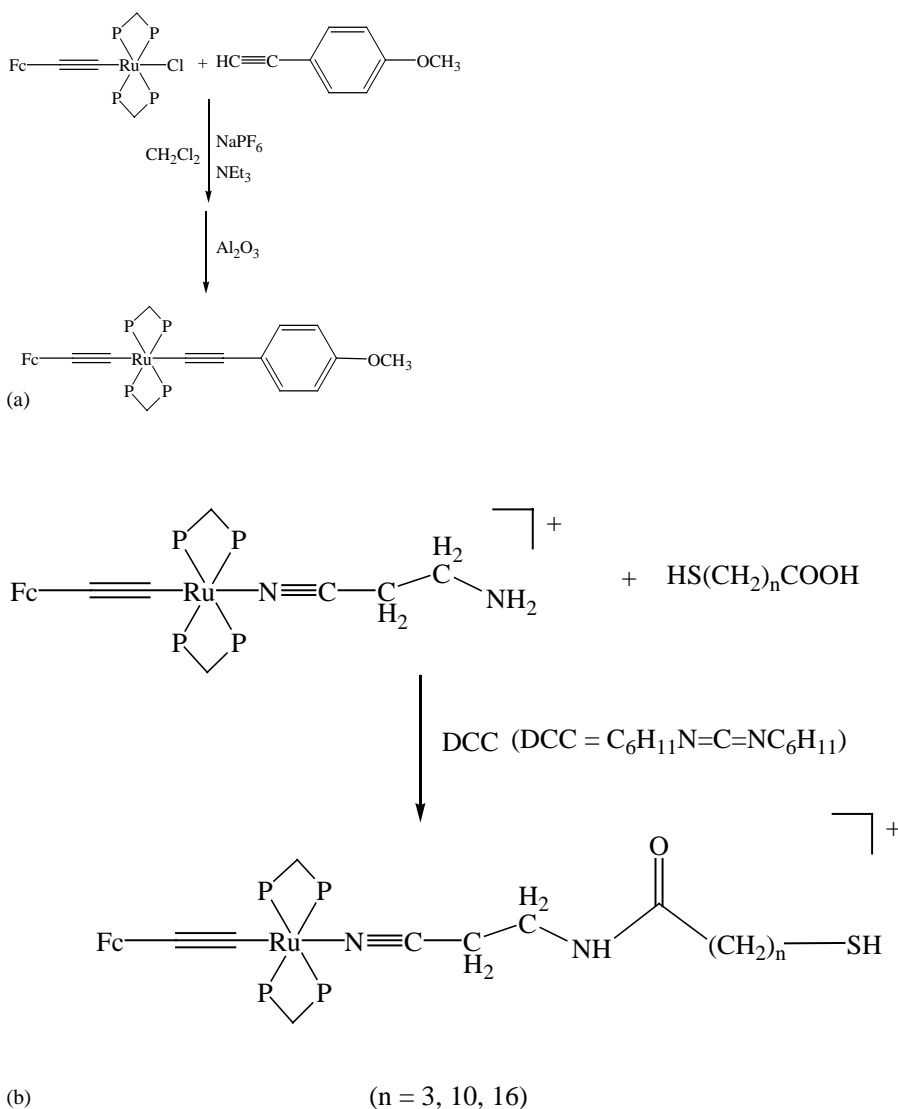


Fig. 3. The schematic diagram of the preparation of (a) FeRu(OCH₃) for Si surface (b) FeRu(SH) for Au surface.

surface, the p-type Si (111) sample of size 10 mm × 4 mm and thickness 0.6 mm were used. The samples were first cleaned with acid clean solution (HCl: H₂O₂: H₂O = 1:1:4, RCA2) to remove the metal contamination on the surface and then cleaned with base clean solution (NH₄OH: H₂O₂: H₂O = 1:1:4, RCA1) to remove any organic contamination on the surfaces. To remove the undesired native oxide layer from the Si surface, the cleaned sample was then etched in a buffered oxide etch (BOE) solution for few

seconds and then rinsed with DI water followed by drying with N₂ gas stream. After this treatment, the Si sample is left with 6–8 Å thickness of oxide layer as measured by the ellipsometric method. The DI water rinsing and drying with N₂ were repeated three times just before the STM imaging.

In the case of SiPc molecules, m-SiPc was attached on the Si surface and d-SiPc, which is double-dot-like entities, were attached on the Au surface. Both the m-SiPc and d-SiPc solutions (1 mM) were prepared by dissolving with 2 ml of

CH_2Cl_2 solution in a N_2 atmosphere glove box for about 16 h. Similarly, in the case of $\text{FeRu}(\text{OCH}_3)$ complex attachment on the Si surface, the RCA cleaned samples were soaked in a 1 mM molecule solution for about 36 h. In order to attach the $\text{FeRu}(\text{SH})$ to Au surface, the annealed and well-cleaned Au sample was soaked in a 1 mM molecule solution for about 16 h.

After the molecule attachment on the Si and Au surfaces, the samples were taken out from the molecule solution and washed with the solvent CH_2Cl_2 and cleaned with DI H_2O and dried with N_2 . Then the samples were loaded into the STM chamber immediately in order to determine if the molecules would self-assemble, and also to determine their electronic properties via voltage vs. current (I/V) measurements. The STM measurements were performed in a standard UHV chamber (base pressure 6×10^{-11} Torr) at room temperature using an Omicron micro GmbH STM with W tips that were subject to careful cleaning treatment. All STM data presented in this paper are unfiltered raw data. The polarity of the bias voltage is referred to the tip (i.e., a positive voltage defines tunneling of electrons from the sample to the tip and vice versa). It is important to note that XPS measurements were carried out on these samples after the STM imaging in order to reconfirm the presence of these molecules on the surfaces. The XPS results indicated the presence of these molecules on the surfaces as shown in Fig. 4(a) and (b).

3. Results and discussion

3.1. STM imaging of SiPc monomer and dimer

Fig. 5(a) shows the STM image of m-SiPc on Si surface for a bias voltage of 1.48 V and the set point current of 20 pA. We believe that the bright spots probably correspond to the m-SiPc molecules attached on the Si surface. The experiments were repeated with different tips on the different spots by varying the scan rate under the same conditions. The analysis of these images was done in order to determine the average diameter and the height of the molecule, as well as to find out about

the coverage. From the line profile of this image, we found that, in the case of m-SiPc the average diameter of the spots is about 22 Å and the height of the spot is around 5.4 Å, which is very much in consistent with the theoretical value of m-SiPc [13]. However, it must be noted that although the diameter of most of the bright spots are predominantly around 22 Å, in some images we have also noticed few bright spots smaller or bigger than 22 Å. Hence, we have taken the average of diameter and height of these bright spots, which are indicating that the bright spots correspond to m-SiPc molecules.

Fig. 5(b) shows the image of the d-SiPc molecules on the Au surface, which was obtained with a positive bias of 1.008 V and the set point current of 10 pA. The bright spots are conceivably the d-SiPc on the Au surface. The streaking which is present in the image (parallel to the scan direction) is probably due to the tip-molecule interaction. Having an idea of how many bright spots are present in the entire image, we have calculated their area respect to the area of the total image. These calculations yield an average coverage of about 15% of d-SiPc on the gold substrate. We also noted that in addition to the small bright spots, some of the STM images of d-SiPc on Au substrate also manifest very large bright spots. These are probably conglomerations of many d-SiPc molecules. From the line profile of Fig. 4(b), we find that the average diameter of the white spot is to be around 21 Å and the height of the spot is around 12 Å, which is almost coinciding with the theoretical value of d-SiPc molecule.

3.2. STM imaging of $\text{FeRu}(\text{OCH}_3)$ and $\text{FeRu}(\text{SH})$ complexes

Fig. 6(a) shows the STM image of $\text{FeRu}(\text{OCH}_3)$ complex on Si surface obtained for the bias voltage of 1.6 V with the tunneling current of 20 pA. A careful look on this image revealed that the diameter of the white spot is about 12 Å and the height of this spot is around 20 Å, which is the expected size of this $\text{FeRu}(\text{OCH}_3)$ complex. Fig. 6(b) shows the constant current STM image of the $\text{FeRu}(\text{SH})$ complex on Au(1 1 1) surface for the bias voltage of 1 V with the set point current of

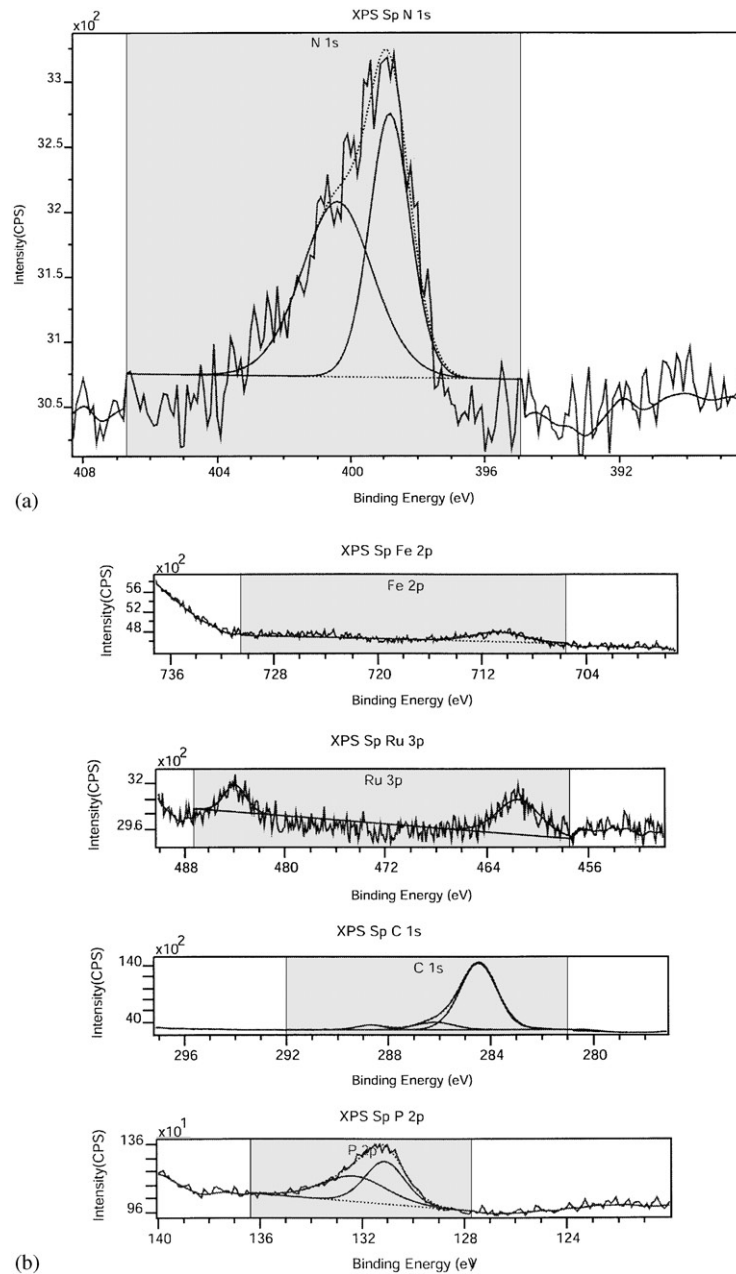


Fig. 4. The XPS data of (a) N 1s peaks observed for m-SiPc on Si surface (b) Fe 2p, Ru 3p, C 1s and P 2p peaks observed for the FeRu(OCH₃) on Si surface.

20 pA. We believe that the white spots observed on this image corresponding to the molecules presence on the surface. The average diameter and the height of this white spot found to be around 12

and 18 Å, respectively, which are the expected values for this molecule.

We have also studied the scanning tunneling spectroscopy (STS) of FeRu(OCH₃) molecule by

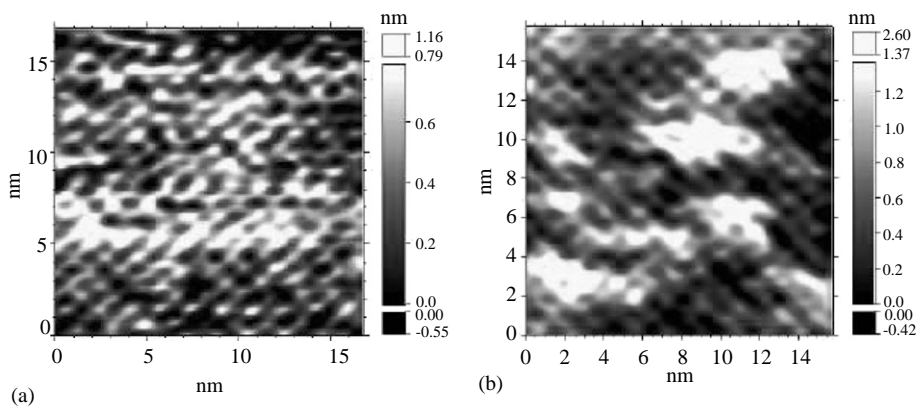


Fig. 5. The constant current STM image of (a) SiPc monomer on Si surface and (b) SiPc dimer on Au surface.

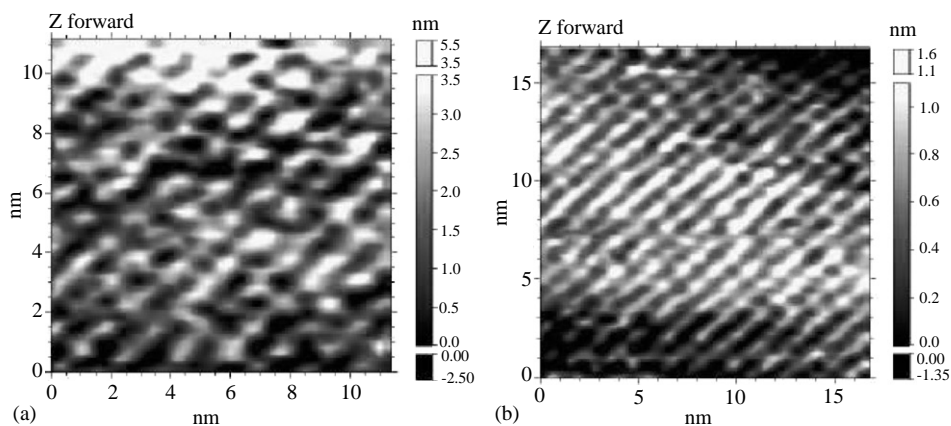


Fig. 6. The constant current STM image of (a) FeRu(OCH₃) on Si surface and (b) FeRu(SH) on Au surface.

keeping the STM tip on the white spot of the STM image of this molecule and sweeping the bias voltage from -4 V to $+4$ V so as to understand the single molecule oxidation by vertical electron transfer. The bias voltage applied between the STM tip and the surface serves as an external tunable perturbation. We have obtained the I/V characteristics at the desired white spot of the image simultaneously with its topography. Upon analyzing different spectroscopic data sets on these molecules, we found that most pixels retain a standard I/V curve derived for electrons tunneling from a tungsten tip into the sample. As shown in Fig. 7(a), a preliminary current–voltage data of this molecule showed that there are two peaks occurred at 3.2 and 3.7 V for the corresponding

tunneling current of 1.2 and 1.24 nA, respectively. We believe that these two peaks correspond to the two oxidation levels, which are expected for this Fe–Ru complex. That is, the cyclic voltammogram (CV) shown in Fig. 7(b) exhibits two reversible oxidation peaks at 0.24 and 0.74 V due to successive oxidation of the Fe and Ru centers. Although absolute voltages of these STS and CV measurements differ because of the difference in the reference voltages and the reference electrodes used in these experiments, but it is significant that the voltage gap difference between the two peaks on both cases of the measurements is 0.5 V. We believe that the reason for these two peaks observed from STS measurements is that when the neutral molecule is imaged and a range of bias

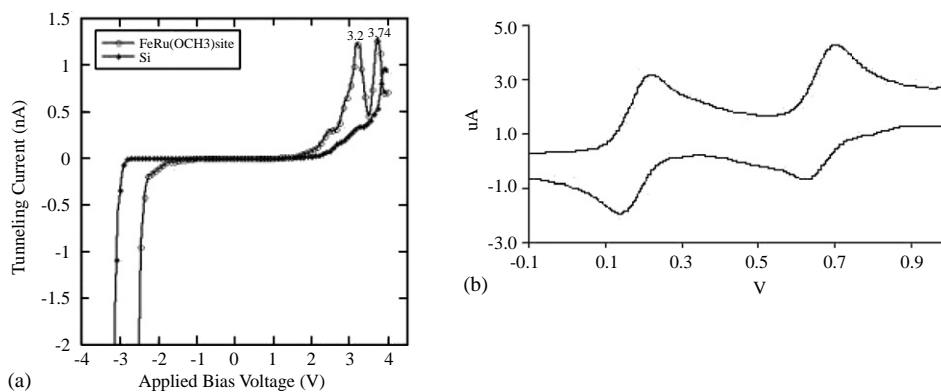


Fig. 7. (a) Current–voltage characteristics of the $\text{FeRu}(\text{OCH}_3)$ molecules on Si surface obtained from STS and (b) cyclic voltammogram of $\text{FeRu}(\text{OCH}_3)$ (100 mV/s), $\text{CH}_2\text{Cl}_2/0.1\text{M TBAPF}_6$ vs. Pt. electrode.

voltage is swept across the molecule, oxidation of this molecule is taking place. However, more experiments are necessary to confirm this prediction as the work on this molecule is still in progress.

4. Conclusions

In conclusion, we have examined the STM studies of the four different kinds of molecules attached with the Au and Si surfaces and the presence of these molecules on the surfaces is confirmed by the XPS characterization studies. Preliminary current–voltage studies have been carried out on $\text{FeRu}(\text{OCH}_3)$ complex in order to find out the vertical electron transfer process. We have observed the two oxidation peaks, which indicate electron transfer from the sample to the tip. STS studies on SiPc molecules and some modification in the $\text{FeRu}(\text{SH})$ complex for $n = 10, 16$ are still in progress. Although more systematic studies are needed to obtain a better understanding of the conduction mechanism in the long alkyl chains in STM, we can conclude that an imaging of the morphology of a Au or Si surface covered with a monolayer of molecule with STM is possible, provided that the tunneling current is sufficiently small. We believe that the Poole–Frenkel effect [14] field enhanced thermal excitation of trapped electrons into the conduction band may provide a possible explanation for this observation. In future, we plan to perform drift

corrected low temperature STM and STS measurements to obtain better resolution of these SiPc and Fe–Ru complex molecules.

Acknowledgements

This work was supported by the Defense Advanced Research Projects Agency, Office of Naval Research, and the National Science Foundation.

References

- [1] C.P. Williams, S.H. Clearwater, *Explorations in Quantum Computing*, Springer, New York, 1988.
- [2] G. Toth, C.S. Lent, *Phys. Rev. A* 63 (2001) 052315-1.
- [3] A.O. Orlov, I. Amlani, R.K. Kummamuru, G. Toth, C.S. Lent, G.H. Bernstein, *Appl. Phys. Lett.* 77 (2000) 295.
- [4] C.S. Lent, *Nature* 288 (2000) 1597.
- [5] Q. Zhang, B. He, Q. Dai, J. Gu, N. Gu, D. Huang, *Supramol. Sci.* 5 (1998) 631.
- [6] D. Touchard, P. Haquette, N. Pirio, L. Toupet, P.H. Dixneuf, *Organometallics* 12 (1993) 3132.
- [7] G.E. Poirier, *Chem. Rev.* 97 (1997) 1117.
- [8] M. Hannack, A. Gul, A. Hirsch, *Mol. Cryst. Liq. Cryst.* 187 (1990) 365.
- [9] M.K. Lowery, A.J. Starshak, J.N. Esposito, P.C. Krueger, M.E. Kenney, *Inorg. Chem.* 4 (1965) 128.
- [10] Z.Y. Li, M. Lieberman, *Supramol. Sci.* 5 (1998) 485.
- [11] Z.Y. Li, M. Lieberman, *Inorg. Chem.* 40 (2001) 932.
- [12] D.W. Dewulf, J.K. Leland, B.L. Wheeler, A.J. Bard, D.A. Batzel, M.E. Kenney, *Inorg. Chem.* 26 (1987) 266.
- [13] Z.Y. Li, M. Lieberman, W. Hill, *Langmuir* 17 (2001) 4887.
- [14] C.A. Mead, *Phys. Rev.* 128 (1962) 2088.